Available online at www.sciencedirect.com
SCIENCE DIRECT®
Journal of Theoretical Biology 222 (2003) 211–218
Journal of Theoretical Biology
www.elsevier.com/locate/jtbi

Biomechanical models of hyphal growth in actinomycetes

Alain Goriely*, Michael Tabor

Program in Applied Mathematics and Department of Mathematics, University of Arizona, Building #89, Tucson, AZ 85721, USA

Received 7 October 2002; accepted 3 December 2002

Abstract

The tip growth of filamentary actinomycetes is investigated within the framework of large deformation membrane theory in which the cell wall is represented as a growing elastic membrane with geometry-dependent elastic properties. The model exhibits realistic hyphal shapes and indicates a self-similar tip growth mechanism consistent with that observed in experiments. It also demonstrates a simple mechanism for hyphal swelling and beading that is observed in the presence of a lysing agent.

Keywords: Tip growth; Filamentary micro-organisms; Bio-elasticity; Large deformation theory

1. Introduction

Filamentary microorganisms are ubiquitous in Nature, and many are conveniently classified as belonging to either the (broadly defined) families of eukaryotic fungi or prokaryotic actinomycetes. Although there are fundamental differences in the internal cellular structure and wall composition of fungi and actinomycetes, they can also exhibit similar morphologies, growth patterns, and mycelial and aerial growth forms. The actinomycetes (which are a loosely defined family of Gram-positive organisms with DNA high in cytosine and guanine content) have been a topic of considerable interest to microbiologists for over a 100 years. As prokaryotes, their internal cellular structure is rather simple: essentially linear nuclear material in a cytoplasmic medium. The cell-wall structure—a topic of intense investigation—is dominated by a network of peptidoglycan polymers. However, the organism is not genomically trivial and the chromosome of a typical streptomycete, such as in *Streptomyces coelicolor* A3(2), is approximately 8 Mbase-pairs long—about twice the size of that found in *Bacillus subtilis*.

An important member of the actinomycete family are the streptomycetes which are of great interest in the pharmaceutical industry because of their ability to generate antibiotics. In a typical growth cycle, the spores bud into long filamentary hyphae which grow in and on the nutrient surface (say a plate of agar). The hyphae undergo branching and a dense mycelium is gradually formed. This phase is usually referred to as the vegetative growth phase. A typical streptomycete filament, such as *S. coelicolor*, is less than 1 μm in diameter and can grow to lengths of 50–100 μm in this phase. A typical example of vegetative growth is shown in Fig. 1. Observations indicate that filamentous growth of actinomycetes is strongly conditioned by both the elastic properties of cellular walls and the physical properties of the environment. Experimental studies of hyphal extension in *S. coelicolor* show that the growth is determined by (Prosser and Tough, 1991):

(i) turgor pressure,
(ii) addition of newly synthesized wall-building material in an apical (tip) extension zone, and
(iii) rigidification of the distal cell wall.

It is generally believed that the wall-building material is transported to the tip by a (not well-understood) diffusive process. The overall picture of hyphal growth is a complex process in which wall-building materials are incorporated into the tip which is stretched by the turgor pressure generated by the intracellular fluid; and as the tip is continually stretched and "rebuilt" the more distant portions of the hyphal wall rigidify. Apical growth in the vegetative phase makes good sense

*Corresponding author. Tel.: +1-520-621-2559.
E-mail addresses: goriely@math.arizona.edu (A. Goriely), tabor@math.arizona.edu (M. Tabor).

0022-5193/03/$ - see front matter
doi:10.1016/S0022-5193(03)00029-8

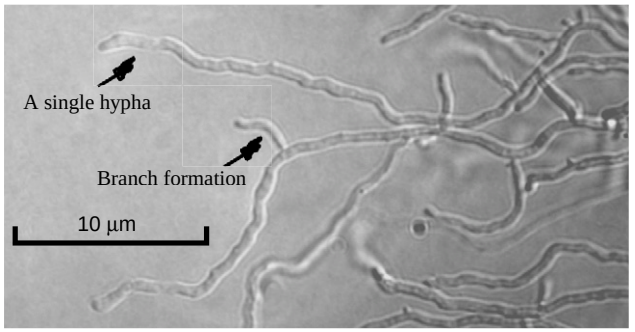

Fig. 1. Mycelial growth of *S. coelicolor* on solid agar medium (microscopy performed at the Imaging Facility, Arizona Research Laboratories, University of Arizona).

energetically since this is more efficient than having to overcome the extra friction with the medium that would be generated if the growth occurred throughout the length of the filament. The vegetative phase is usually followed by a second, aerial, growth phase which can be accompanied by the generation of antibiotics. In this phase, the hyphae grow out of the mycelium, sometimes deforming into helical structures, and ultimately break up into spores—which then begin the vegetative growth cycle again. It should be noted that aerial hyphal growth is no longer confined to the tip.

Filamentary fungi are typically at least an order of magnitude bigger than the streptomycetes and, as eukaryotes, have a much more complex internal structure which includes a cytoskeleton, membrane-bound organelles, etc. The cell-wall structure is different from the actinomycetes and consists, loosely speaking, of stiff chitin molecules embedded in a polymer complex (Wessels, 1990). Despite all these differences, tantalizing morphological similarities between the filamentary organisms remain, especially that of hyphal growth at the tip of the organism. While it is generally accepted that turgor pressure is the primary driving force for actinomycetes, its role in the growth of fungi is still a topic of debate (Money, 1997) and the cytoskeleton almost certainly plays some role in straining the cell membrane and transporting the wall-building materials to the tip.

The modeling of tip growth in both families of organisms has inevitably been a topic of interest for some time. These models can be conveniently classified as either "geometrical" or "biomechanical." Essentially, the former class of models balance the increase in wall area of an advancing membrane tip with the incorporation of wall-building material. Models by Trinci and Saunders (Saunders and Trinci, 1970; Trinci and Saunders, 1977) consider the consequences of having a given tip shape such as a hemisphere or an ellipse (the latter proving to be more realistic than the former). An early attempt at a geometrical model was also investigated by da Riva Ricci and Kendrik (1972). An interesting model of fungal growth is due to Bartnicki-Garcia et al. (1989) who derived an explicit mathematical form for hyphae advancing with a given constant velocity. In a separate paper (Goriely et al., 2002), we give a more mathematical examination of such geometrical models. Biomechanical models to date, such as those developed by Koch (1995), draw on concepts from shell theory and the Young–Laplace law for membranes, and suggest connections between experimentally observed tip shapes and their material properties. An excellent review of hyphal growth dynamics from the biological perspective has been given by Prosser and Tough (1991).

Here we concentrate on turgor pressure driven apical growth of actinomycetes, and using large deformation elasticity theory (Green and Adkins, 1970), develop a self-consistent, three-dimensional, biomechanical model in which the cell wall is modeled as a stretchable and growing elastic membrane with geometry-dependent moduli. This model is capable of producing realistic tip shapes and demonstrates that there is not so much one special tip shape but rather that the tip expansion is essentially *self-similar*. The introduction of a shell modulus with a coordinate dependence provides a simple biophysical representation of the old, but widely accepted, "soft-spot" hypothesis of Reinhardt (1892) in which the hyphal tip is considered to be more stretchable than more distal regions which become asymptotically rigid. This model is also able to provide a simple, but biophysically credible, description of tip swelling and beading observed in the presence of a lysing agent, and a simple scaling relationship between the modulus and the (turgor) pressure clarifies some of the interpretations of these phenomena.

2. Governing equations

To model the biomechanical features of tip growth, we begin by considering an extensible axisymmetric elastic membrane filled with an incompressible viscous fluid under pressure and neglect shear and bending resistance. This type of formulation has been used successfully to describe the shape of red blood cells and other biomembranes (Skalak et al., 1973; Secomb and Gross, 1983) and we adapt it here to include the effects of pressure-induced stretch, growth, and geometry-dependent elastic properties of the membrane. We assume that the shape of the membrane remains axisymmetric in the deformation. As shown in Fig 2, the membrane surface $\mathscr{S}$ is defined by revolving a planar curve $\mathscr{C}$ around the z-axis. The planar curve $\mathscr{C}$ is parameterized by the material coordinate σ counted from the intersection $\mathscr{O}$ of the surface with the z-axis. The shell geometry is characterized by the coordinates $r = r(\sigma)$ and $\theta = \theta(\sigma)$, where $\theta(\sigma)$ is the angle between the normal to $\mathscr{C}$ at σ and the z-axis. The arclength

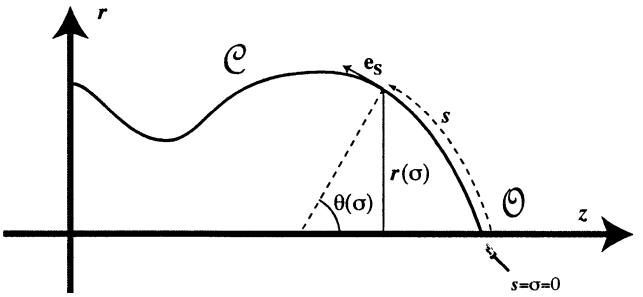

Fig. 2. The curve $\mathscr{C}$ with the coordinates $(r(\sigma), \theta(\sigma))$.

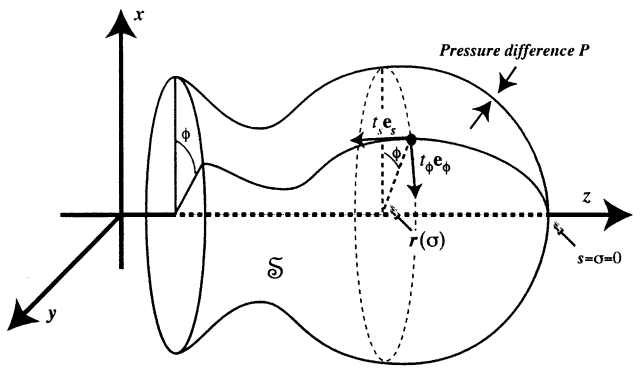

Fig. 3. The surface $\mathscr{S}$ with stresses (t_s, t_φ).

$s = s(\sigma)$ is measured from $\mathscr{O}$. Before deformation or growth, the material parameter σ is identified with the arclength, and the initial shell configuration is referred to as the reference configuration. If we consider axisymmetric deformation of the surface, we can define the *radial stretch ratio*

$$\lambda_\varphi = \frac{r}{r_0}, \tag{1}$$

at a given (material) point as the ratio between the original radius r_0 at that point and the new radius r, and the extensional *stretch ratio*

$$\lambda_s = \frac{\partial s}{\partial \sigma}, \tag{2}$$

as the amount of stretching of the body coordinates with respect to arclength. These two *extension ratios* $(\lambda_\varphi, \lambda_s)$ completely define the deformation of an axisymmetric reference shape. We now define the stresses acting on the membrane surface: let t_s be the tension on the surface along the tangent $\mathbf{e}_s$, in the direction of increasing arclength; and let t_φ be the tension along the unit vector $\mathbf{e}_\varphi$, normal to $\mathbf{e}_s$ in a plane tangent to $\mathscr{S}$, and in the direction of increasing azimuthal angle φ (see Fig. 3). The equations for mechanical equilibrium for a surface of revolution in the normal and tangential direction are thus, respectively (Evans and Skalak, 1980),

$$P = \kappa_s t_s + \kappa_\varphi t_\varphi, \tag{3}$$

$$\frac{\partial (r t_s)}{\partial s} - t_\varphi \frac{\partial r}{\partial s} + r\tau_c = 0, \tag{4}$$

where

$$\kappa_\varphi = \frac{\sin\theta}{r} \quad \text{and} \quad \kappa_s = \frac{\partial \theta}{\partial s} \tag{5}$$

are the principal membrane curvatures, P is the pressure difference across the membrane, and τ_c is the shear stress on the membrane. This last term could be taken to represent the drag forces exerted by the surrounding nutrient medium on the growing filament. Appropriate modeling of this effect is non-trivial and will be left to future work. For now, as with other models of hyphal growth, this term will be set to zero in our analysis. The two equations [(3), (4)] can be written in terms of r and θ by using the geometric relation $\mathbf{e}_s = \cos\theta \mathbf{e}_r + \sin\theta \mathbf{e}_z$, and $\partial\theta/\partial s = \kappa_s$, and take the form

$$t_s \frac{\partial \theta}{\partial s} + \frac{\sin\theta}{r} t_\varphi = P, \tag{6}$$

$$\frac{\partial t_s}{\partial s} = \frac{\cos\theta}{r}(t_\varphi - t_s). \tag{7}$$

In the case of constant pressure P we show in the appendix that there is an integral of Eqs. (6) and (7), i.e. a function of the variables constant along the curve $\mathscr{C}$, given by

$$C = r^2(2t_s\kappa_\varphi - P). \tag{8}$$

In particular, for all solutions $(r(\sigma), \theta(\sigma))$ crossing the z-axis, we have $C = 0$.

We can now relate stresses to strains by introducing a strain–energy function that describes the elastic properties of the membrane. Here, we use large deformation theory and relate the components of the material strain tensor to the extension ratios (Evans and Skalak, 1980):

$$e_{ss} = \tfrac{1}{2}(\lambda_s^2 - 1), \tag{9}$$

$$e_{\varphi\varphi} = \tfrac{1}{2}(\lambda_\varphi^2 - 1). \tag{10}$$

We model the cell wall as a linear elastic membrane. The elastic properties of bacterial walls are not sufficiently understood to warrant the use of higher order models and a linear relationship is more than adequate for the current investigation. The analysis presented here does not rely significantly on this particular choice of constitutive relationship and can be easily adapted to other cases. In the linear case, the stress–strain relations are simply given by expressions of the form (Skalak et al., 1973):

$$t_s = Ae_{ss} + Be_{\varphi\varphi}, \tag{11}$$

$$t_\varphi = Ae_{\varphi\varphi} + Be_{ss}, \tag{12}$$

where A and B characterize the elastic properties of the membrane. Note that these "moduli" can be a function of the material parameter σ. In terms of the extension ratios, the stress–strain relation can be

written as

$$t_s = A\lambda_s^2 + B\lambda_\varphi^2 - (A+B) = A(\lambda_s^2 + \mu\lambda_\varphi^2 - (1+\mu)), \quad (13)$$

$$t_\varphi = A\lambda_\varphi^2 + B\lambda_s^2 - (A+B) = A(\lambda_\varphi^2 + \mu\lambda_s^2 - (1+\mu)), \quad (14)$$

where $\mu = B/A$ is a measure of the ratio of extensibility of the membrane in the azimuthal and longitudinal directions.

Taking advantage of the constant (8), we can derive through elementary manipulation, a closed system for the membrane variables $(r(\sigma), \theta(\sigma))$:

$$\frac{\partial r}{\partial \sigma} = \lambda_s \cos\theta, \quad (15)$$

$$\frac{\partial \theta}{\partial \sigma} = -\left(\frac{\lambda_s}{r}\right)\frac{\sin\theta[r^2 - r_0^2(1+\mu(1-\lambda_s^2)] - prr_0^2}{r^2\mu - r_0^2(1+\mu-\lambda_s^2)}, \quad (16)$$

where $p = P/A$ is an "effective" pressure and, assuming $C = 0$, it follows from Eq. (8) that

$$\lambda_s^2 = 1 + \mu(1 - (r/r_0)^2) + rp/(2\sin\theta). \quad (17)$$

These equations describe the deformation of a stretchable axisymmetric elastic membrane defined relative to the reference shape $r_0(\sigma)$, and with elastic parameters $(\mu, A(\sigma))$ under pressure P. A complete picture of the cell geometry is conveniently obtained by integrating two auxiliary equations:

$$\frac{\partial z}{\partial \sigma} = \lambda_s \sin\theta, \quad (18)$$

$$\frac{\partial s}{\partial \sigma} = \lambda_s, \quad (19)$$

with boundary values $z(L) = 0$ (L is a reference length taken as the total longitudinal length of the membrane) and $s(0) = 0$, thereby enabling one to directly plot out the shell shape $(r(\sigma), z(\sigma))$ and obtain information about the distance $s(\sigma)$ of any material point σ from the apex.

It is generally accepted that growth in actinomycetes takes place in the apical region where the cell walls are softer. The softening of cell walls close to the tip can easily be taken into account by using a material-dependent elastic function $A = A(\sigma)$ fitted from published data on the rate of incorporation of tritiated *N*-acetyl *D*-glucosamine along the hyphae of *S. coelicolor*. A3(2) (Gray et al., 1990). The general form of $p = P/A$ that we choose is

$$p = \frac{P}{2}\left[1 - \tanh\left(\frac{\sigma - \sigma_1}{\alpha}\right)\right] + \beta, \quad (20)$$

where P is the turgor pressure and the parameters σ_1 and α describe the length of the apical extension zone. Since $\lim_{\sigma\to\infty} p = \beta$, the parameter β describes the effective pressure in distal regions. A typical plot of $p(\sigma)$ is shown in Fig. 4. It is important to note that in our model the critical parameters of pressure and modulus only appear in the ratio P/A. Thus, a decreased modulus or increased pressure (or vice versa) are, at the mechanical level, indistinguishable. We will return to this point is our discussion of lysis. We also comment that the idea of a geometry-dependent elastic modulus is biophysically plausible: classic results in polymer physics (Treloar, 1975) tell us (at least in the case of rubbers) that the modulus increases with the degree of polymeric cross-linking, and in the current context this is consistent with the process of wall rigidification.

Finally, we need to consider how to incorporate a "growth" mechanism into the current model. At the biochemical level, the growth process comes about through a continuous and complex process by which wall-building polymers are transported to, and incorporated into, the extended tip. At the biomechanical level the effect of growth can be included, quite simply, by a re-parametrization of the extended membrane. The idea is that since the walls of the filament are regenerated in the growth process in the apical region (and rigidified in the distal region) they are again susceptible to applied stresses (the turgor pressure) and can be further stretched. That is, growth is modeled by a re-parameterization of the surface once mechanical equilibrium is reached. Without re-parameterization the membrane would, for a fixed pressure, remain in its equilibrium configuration. This procedure is implemented in the following way as illustrated in Fig 5. We start with an initial shape defined by the function $r_0(\sigma)$, $0 \leqslant \sigma \leqslant L_0$, and compute the new shape $r(\sigma)$ by solving the system (15)–(16) subject to the boundary condition $r(L_0) = R_0$, $r(0) = 0$. The new shape $r(\sigma)$ represents the new mechanical equilibrium of the membrane. The effect of growth is achieved by recomputing a new reference shape $r_1(\sigma) = r(s)$, where, $s = s(\sigma)$ is the arclength along the stretched curve with new length $L_1 = s(L_0)$ computed from Eq. (19). The shape $r_1(\sigma)$ is then used to

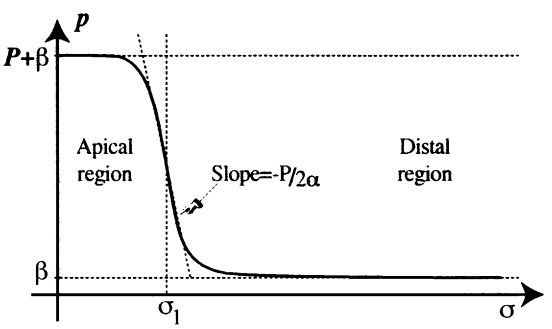

Fig. 4. A typical plot of the renormalized pressure $p = P/A(\sigma)$. Close to the tip ($\sigma = 0$), the walls are soft and the elastic coefficient minimal. In the distal regions, the walls are set and the elastic coefficient A is, comparatively, very large, so that the effective pressure is small (equal to β).

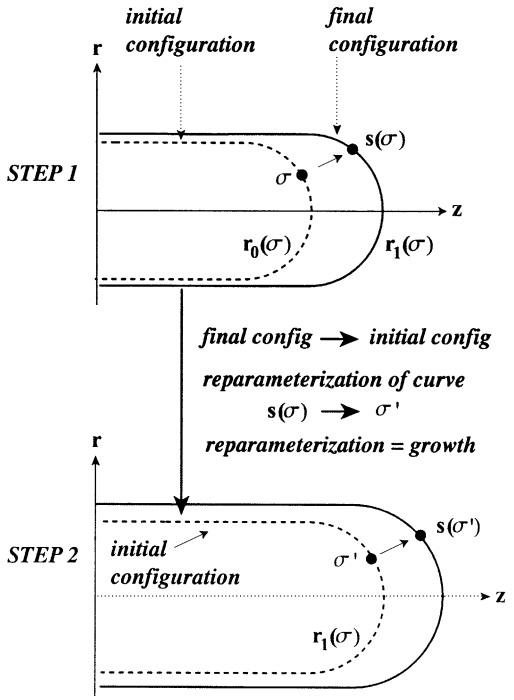

Fig. 5. Schematic representation of the re-parameterization/growth process.

compute a new mechanical equilibrium with boundary conditions $r(L_1) = R_0$, $r(0) = 0$ and so on. More complicated growth models can easily be implemented. In general, we can specify a material re-parameterization of the stressed surface by specifying a function $\tilde{\sigma} = \tilde{\sigma}(\sigma, r(\sigma), \theta(\sigma), \lambda_s)$ consistent with the underlying growth process (Rodriguez et al., 1994; Taber, 1995; Chen and Hoger, 2000). Once this function is specified, the stressed surface is re-parameterized and the corresponding (virtual) new unstressed shape is recomputed by solving Eq. (17) for the unstressed profile. Once the new unstressed shape is known, one can compute a new stressed shape $r_1(\sigma)$ and repeat this process. However, in the present analysis, we use a simple growth model consistent with the observation that addition of newly synthesized wall material occurs in the extension zone.

This approach, namely elastic response combined with surface re-parameterization to simulate wall rebuilding, enables us to generate growth of the membrane within the framework of "pure" elasticity. We are tempted to term this process "morpho-elasticity" to distinguish it from descriptions of membrane growth that involve concepts (in the traditional rheological sense) of visco-elastic and/or plastic deformation. For example, the latter description offers irreversible medium flow beyond a critical stress, and is one way of producing "growth", even without membrane regeneration. Ultimately, the model, and choice of terminology, should be determined by a proper understanding of the membrane properties and the growth processes involved. Here, we simply show that the chosen biomechanical model is able to generate realistic hyphal expansion.

3. Results: hyphal growth, lysis and beading

The computation of a growth profile requires a dedicated numerical scheme due to the highly sensitive nature of the boundary conditions and the chosen model of growth. It is performed as a discrete sequence of boundary value problems and time-evolution is performed, as described above, by re-parameterization of the initial profile $r_0(s)$. A typical computation is shown in Fig. 6. A three-dimensional graphic of the same computation is shown in Fig. 7. Two remarkable observations come out of these computations. First, the same asymptotic shape is obtained from different initial profiles and seems to depend only on the elastic parameters and pressure. Given that the moduli and the growth law are geometry dependent it is not necessarily obvious that this would be the case. Second, the tip shape, once established is effectively *self-similar*, that is at each step the new shape is a duplicate of the previous one properly translated (see Fig. 8). A variety of other computations (not displayed here) all show that if the tip expansion is concentrated at the tip, as embodied through the choice of an effective pressure function such as Eq. (20), the same growth phenomenology is displayed. A theoretical analysis of these self-similar shapes is presented in Goriely and Tabor (2002). An important quantity to track is the total area of the membrane given by

$$Area = \int_0^L 2\pi r \lambda_s \, d\sigma. \tag{21}$$

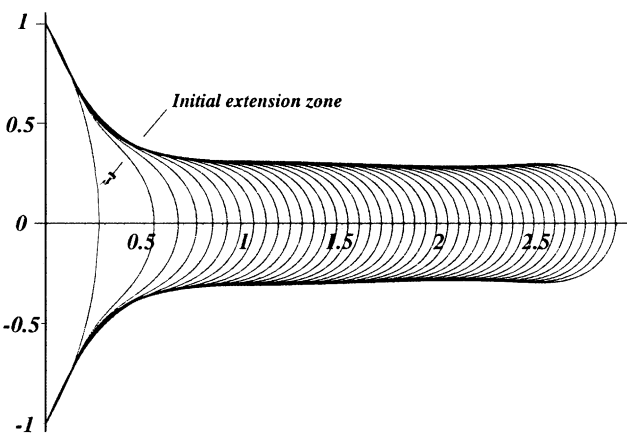

Fig. 6. Sequence of growth obtained from an initial spherical shape of radius 2. The parameters used are $\mu = 1/2$, $\sigma_1 = \pi/12$, $P = 1$, $\alpha = 1/8$, $\beta = 10^{-6}$. The computation is the result of 200 iterations (every 5 shown).

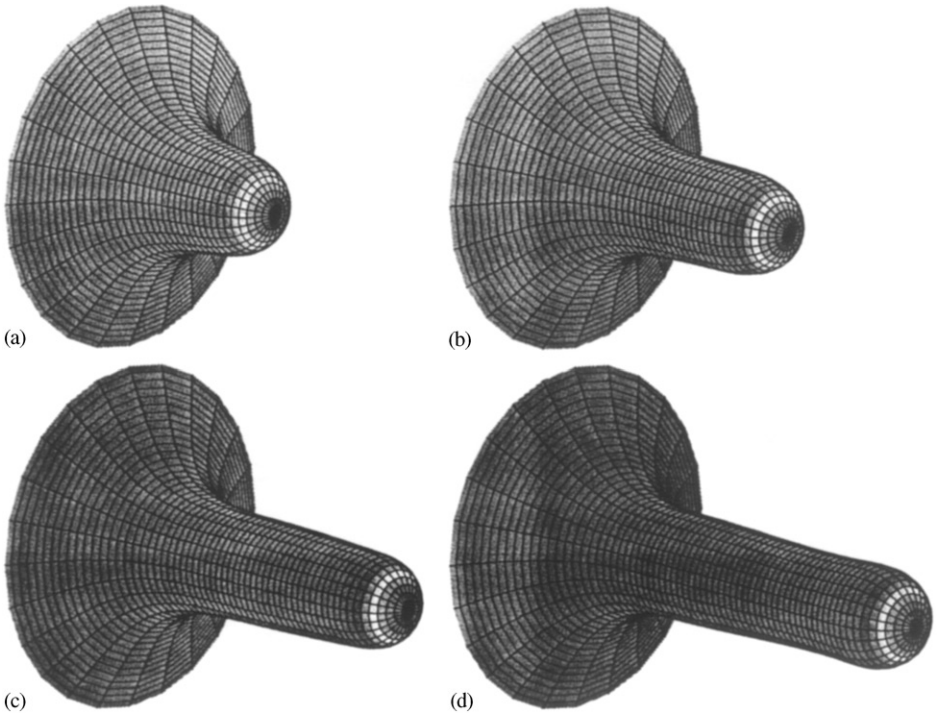

Fig. 7. Three-dimensional version of Fig. 6 (iterates 50, 100, 150 and 200 shown).

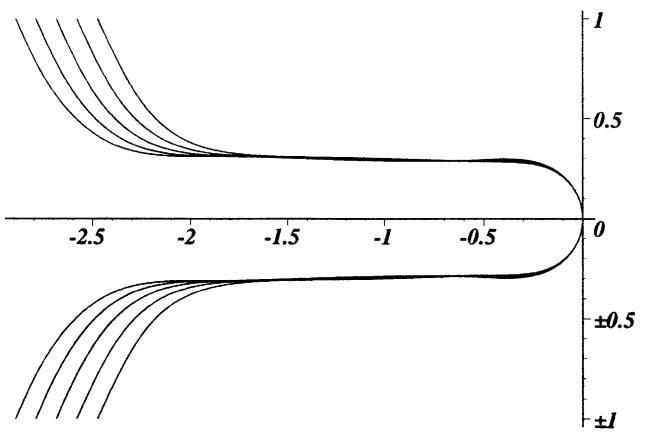

Fig. 8. The same growth sequence as shown in Fig. 6 but in the reference frame of the tip (iterates 160–200 shown).

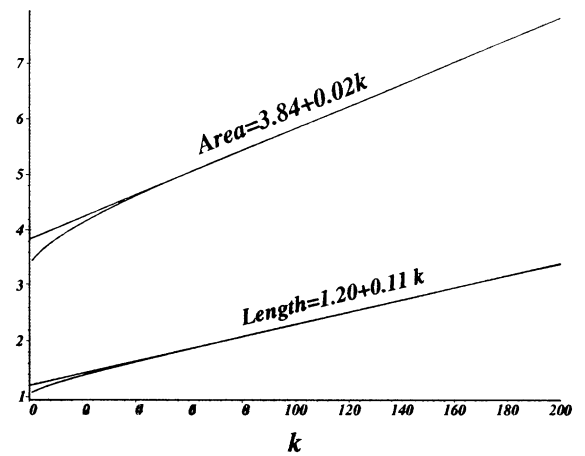

Fig. 9. Increase of total length and area during growth (as a function of the number of growth iterates k). After an initial phase, the increase of length and area is linear with growth (as observed in experiments).

The change of length and area during growth is shown in Fig. 9.

As a further qualitative test of the validity of our model, we can consider two simple situations where modification of the elastic properties of cell walls lead to change in morphology. First, when the hyphae are treated with β-lactam antibiotics, the rigidification of the wall is partly prevented resulting in *apical swelling*. This effect is described as an "...increase internal hydrostatic pressure acting on a cell wall of reduced rigidity" (Prosser and Tough, 1991); in our setting, we see that both effects are represented by an increase of the effective pressure parameter p (see Fig. 10). If the hyphae are treated instead with lysozyme, the hyphae can exhibit *beading*, that is generalized non-localized hyphal swelling as shown in Fig. 11. Again, this situation can be easily modeled by a variation of the parameter p along the hyphae. A typical example of such a profile is shown in Fig. 12. Here the big dips in p correspond to a large increase in the elastic modulus—since the beading is believed to be

associated with septation, one would expect a significant increase in structural rigidity in the neighborhood of the septa that would survive the introduction of lysozyme.

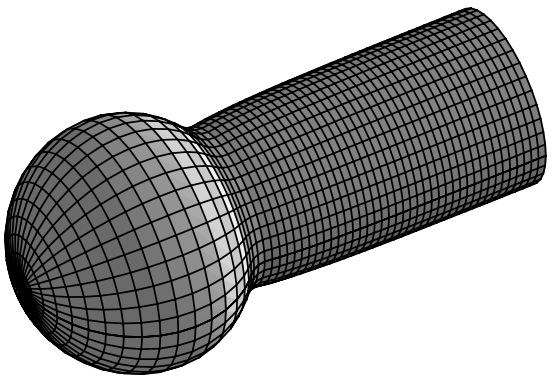

Fig. 10. Apical swelling obtained by increase in the parameter p.

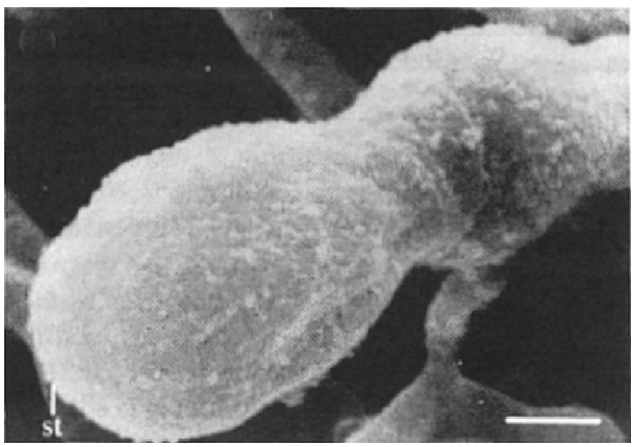

Fig. 11. Beading: a swollen hyphal *S. coelicolor* tip (st). The tip is approximately 2–5 μm in diameter and its surface appears roughened due to the lytic action of lysozome. Bar: 1 μm. (Picture Courtesy of J. I. Prosser.)

4. Conclusions

The formulation presented here is sufficiently general to accommodate many different effects such as external stress (produced for instance by the medium), varying elastic moduli, and more general strain–energy functions describing the elastic response of the cell walls (Skalak et al., 1973). A natural question is whether this type of theoretical framework can be used to model the morphologically similar, but biochemically very different, process of hyphal growth in filamentary fungi. Although role of turgor pressure and cytoskeletal structure in the expansion process is not completely clear (Money, 1997), it is important to note that at the biomechanical level, *all* the normal stresses are balanced through relation (3). Thus, while we have referred to P as the pressure difference across the membrane it is, more correctly, the sum of all the external normal forces which, in addition to the difference between the external pressure and intracellular fluid pressure, can include the net normal forces generated by the cytoskeleton on the cell wall. With this consideration in mind we can see that our biomechanical description of apical expansion is applicable even in the case of no, or negligible, turgor pressure. Furthermore, the equation of balance for tangential forces (4) can include the effect of external surface stresses, τ_e. While such a term has been neglected here, it could be included to represent friction between the growing hypha and its surrounding medium. It could also be used to represent, if present, any tangential stresses exerted by the cytoskeleton on the cell wall. In many fungi, tip growth seems to occur by incorporation of material synthesized in distal regions and transported to the tip by membrane-bound vesicles (Gooday and Trinci, 1980) (as opposed to the probable diffusive process in actinomycetes). Although our re-parameterization approach to wall regeneration cannot (nor, indeed, wishes to) simulate this level of biochemical detail, it can still capture the essence of a continuous wall-building process.

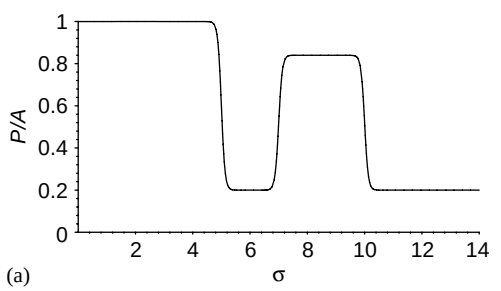

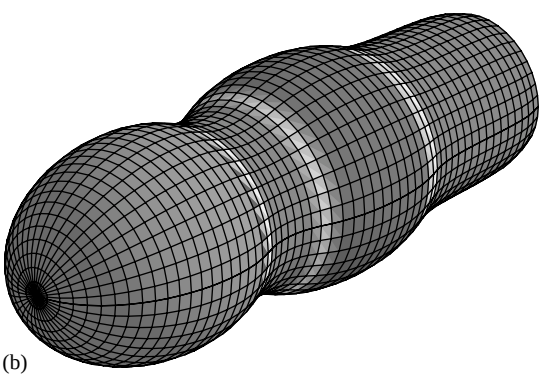

Fig. 12. (a) Effective pressure profile capable of reproducing lysozyme-induced beading. (b) Beading obtained by allowing variations of p along the hyphae.

Acknowledgements

The authors wish to thank Liz Wellington (University of Warwick) for introducing them to this problem and for supplying a variety of bacterial samples; and David Bentley (Imaging Facility, Arizona Research Laboratories, University of Arizona) for his considerable help in imaging hyphal growth data. A. G. is supported by the Sloan Foundation and a Faculty Small Grant from the University of Arizona. M.T. was partially supported by National Science Foundation Grant DMS-9704421.

Appendix

In order to derive the constant (8) it is convenient to collect together the governing equations in the form

$$P = k_s t_s + k_\varphi t_\varphi, \tag{A.1}$$

$$\frac{\partial(rt_s)}{\partial s} = t_\varphi \cos\theta, \tag{A.2}$$

$$\frac{\partial r}{\partial s} = \cos\theta, \tag{A.3}$$

where k_s, k_φ are given in Eq. (5). From Eq. (5) we easily see the purely geometric relationship

$$\frac{\partial(rk_\varphi)}{\partial s} = k_s \frac{\partial r}{\partial s}. \tag{A.4}$$

On multiplying both sides of (A.1) by $\partial r/\partial s$ and using (A.4) it follows that

$$t_s \frac{\partial(rk_\varphi)}{\partial s} + k_\varphi t_\varphi \frac{\partial r}{\partial s} = P \frac{\partial r}{\partial s}. \tag{A.5}$$

From (A.2) and (A.3) we observe that

$$\frac{\partial(rt_s)}{\partial s} = t_\varphi \cos\theta = t_\varphi \frac{\partial r}{\partial s}, \tag{A.6}$$

and hence

$$k_\varphi t_\varphi \frac{\partial r}{\partial s} = k_\varphi \frac{\partial(rt_s)}{\partial s}. \tag{A.7}$$

Eq. (A.5) can now be written as

$$t_s \frac{\partial(rk_\varphi)}{\partial s} + k_\varphi \frac{\partial(rt_s)}{\partial s} = P \frac{\partial r}{\partial s}, \tag{A.8}$$

and on multiplying both sides by r this can be re-expressed in the form

$$\frac{\partial(r^2 t_s k_\varphi)}{\partial s} = Pr \frac{\partial r}{\partial s}. \tag{A.9}$$

Integrating both sides with respect to s gives

$$r^2 t_s k_\varphi = \int Pr \frac{\partial r}{\partial s} + C = \int Pr \, \mathrm{d}r + C, \tag{A.10}$$

and hence

$$t_s k_\varphi = \frac{1}{r^2} \int Pr \, \mathrm{d}r + \frac{C}{r^2}, \tag{A.11}$$

where C is the constant of integration. Thus, for constant pressure $P = P_0$ we have

$$C = r^2(t_s k_\varphi - \tfrac{1}{2}P_0). \tag{A.12}$$

References

Bartnicki-Garcia, S., Hergert, F., Gierz, G., 1989. Computer simulation of fungal morphogenesis and the mathematical basis for hyphal tip growth. Protoplasma 153, 46–57.

Chen, Y., Hoger, A., 2000. Constitutive functions of elastic materials in finite growth and deformation. J. Elasticity 59, 175–193.

da Riva Ricci, D., Kendrik, B., 1972. Computer modelling of hyphal tip growth in fungi. Can. J. Bot. 20, 2455–2462.

Evans, E.A., Skalak, R., 1980. Mechanics and Thermodynamics of Biomembranes. CRC Press, Inc, Boca Raton, FL.

Gooday, G.W., Trinci, A.P.J., 1980. Wall structure and biosynthesis in fungi. In: Gooday, G.W., Lloyd, D., Trinci, A.P.J. (Eds.), The Eukaryote Microbial Cell. Cambridge University Press, London, pp. 207–251.

Goriely, A., Tabor, M., 2002. Self-similar tip growth in filamentary organisms. Phys. Rev. Lett., submitted for publication.

Goriely, A., Karolyi, G., Tabor, M., 2002. Growth induced curve dynamics for filamentary micro-organisms Phys. Rev. E., in press.

Gray, D.I., Gooday, G.W., Prosser, J.I., 1990. Apical hyphal extension in *Streptomyces coelicolor* A3(2). J. Gen. Microbiol 136, 1077.

Green, A.E., Adkins, J.E., 1970. Large Elastic Deformations. Clarendon Press, Oxford.

Koch, A.L., 1995. The problem of hyphal growth in streptomycetes and fungi. In: Koch, A.L. (Ed.), Bacterial Growth and Form. Chapman & Hall, New York, pp. 137–150.

Money, N.P., 1997. Wishful thinking of turgor revisited: the mechanics of fungal growth. Fungal Genet. Biol. 21, 173–187.

Prosser, J.I., Tough, A.J., 1991. Growth mechanisms and growth kinetics of filamentous microorganisms. Crit. Rev. Biotechnol. 10, 253–274.

Reinhardt, M.O., 1892. Das wachsthum der Pilzhyphen. Jahrb. Wiss. Bot. 23, 479–566.

Rodriguez, E.K., Hoger, A., McCulloch, A., 1994. Stress-dependent finite growth in soft elastic tissue. J. Biomech. 27, 455–467.

Saunders, P.T., Trinci, A.P.J., 1970. Determination of tip shape in fungal hyphae. J. Gen. Microbiol. 110, 469–473.

Secomb, T.W., Gross, J.F., 1983. Flow of red blood cells in narrow capillaries: role of membrane tension. Int. J. Microcirc: Clin. Exp. 2, 229–240.

Skalak, R., Tozeren, A., Zarda, R.P., Chien, S., 1973. Strain energy function of red blood cell membranes. Biophys. J. 13, 245–264.

Taber, L., 1995. Biomechanics of growth, remodeling and morphogenesis. Appl. Mech. Rev. 48, 487–545.

Treloar, L.R.G., 1975. The Physics of Rubber Elasticity. Clarendon Press, Oxford.

Trinci, A.P.J., Saunders, P.T., 1977. Tip growth of fungal hyphae. J. Gen. Microbiol. 103, 243–248.

Wessels, J.G.H., 1990. Role of cell wall architecture in fungal tip growth generation. In: Heath, I.B. (Ed.), Tip Growth in Plant and Fungal Cells. Academic Press, San Diego.